Prediction of Extreme Ship Responses

Using Potential Flow and RANSE Codes

Ould M. El Moctar
Germanischer Lloyd

ABSTRACT

The paper presents numerical procedures to simulate ship seakeeping responses involving extreme motions and loads. Potential-flow codes are needed for a statistic/probabilistic long-term analysis of the ship's operation to define representative or most critical environmental conditions. Then a RANSE solver is employed to model highly nonlinear ship-wave interaction by solving the nonlinear rigid body six degrees of motion equations in the time domain. Extreme ship motions and wave-induced loads, including impact-related effects caused by slamming and green water on deck, can be computed simultaneously. Various applications for different ship types show the capability of the numerical simulations.

KEYWORDS

RANSE; ship motions; ship seakeeping

INTRODUCTION

For many seakeeping issues, seakeeping is determined as follows:

- Representation of the natural seaway as superposition of many regular (harmonic) waves
- Computation of the ship responses of interest in these harmonic waves

Addition of the reactions in all these harmonic waves to a total reaction (superposition)

This simplified linear approach is appropriate for many questions in ship seakeeping and frequently applied. The corresponding tool at Germanischer Lloyd (GL) is a 3-d Green function method (GFM). The advantage of this approach is that it is very fast and allows thus the investigation of many parameters (frequency, wave direction, ship speed, metacentric height, etc.). Computations become considerably more expensive if this simplification is not made. Non-linear computations are usually necessary for the treatment of extreme motions; here simulation in the time domain is the proper tools. Germanischer Lloyd uses nonlinear time-domain strip theory codes such as GL ROLLS and GL SIMBEL, Söding (1982), Pereira, (1988), Brunswig et al (2006). Methods that directly solve the Reynolds-averaged Navier-Stokes equations (RANSE), possibly including the two-phase flow of water and air, are better able to describe the physics associated with water on deck, viscous damping, 3d-effects etc. However, the computational effort for a three-dimensional RANSE method to simulate motions and loads on a ship at small, successive instances of time over a long time period appears beyond current computational capabilities

Combining intelligently potential flow methods with RANSE simulations allows exploiting the respective strengths of each approach, El Moctar et al. (2004, 2005). The approach starts with a potential flow code analysis to identify the most critical parameter combination for a ship response. Then a RANSE analysis determines the ship motions and loads.

This paper presents a numerical procedure based on the combined use of a boundary element method (BEM), a statistical analysis us-

ing random process theory and an extended RANSE solver to obtain the structural response of ships in a seaway. The BEM obtained the hydrodynamic data base, needed for a statistic/probabilistic long-term analysis of the ship's operation to obtain so-called equivalent regular design waves that represented design load conditions. The extended RANSE solver then obtained ship motions and the corresponding pressures distribution acting on the ship subject to these design wave conditions by solving the nonlinear rigid body six degrees of motion equations in the time domain. Wave-induced loads, including impact-related effects caused by slamming and green water on deck, were computed simultaneously. The resulting hydrodynamic pressures were transformed into nodal forces and became part of the input for the FE code.

The computational procedure has been applied to a large variety of ships, e.g. El Moctar et al. (2004, 2006), Some applications involving extreme responses are presented here.

THE EXTENDED RANSE SOLVER

The RANSE solver Comet implements interface-capturing techniques of the volume-of-fluid (VOF) type. The solution domain is subdivided into a finite number of control volumes that may be of arbitrary shape. The spatial distribution of each of the two fluids is obtained by solving an additional transport equation for the volume fraction of one of the fluids.

Fluid structure interaction effects were presently not fully accounted for. Except for the investigation of hull girder whipping, the ships were assumed to be rigid bodies. The fluid was assumed to be viscous and incompressible. The nonlinear ship motion equations were solved and coupled to the RANSE solver. The computational procedure comprised the following steps:

- The RANSE-solver computed the flow around a ship's hull, taking into account viscosity, turbulence, and deformation of the free surface.
- Hydro- and aerodynamic forces and moments acting on the ship were calculated by integrating the pressure and friction stresses over the ship's surface.

The nonlinear equations of the rigid body six degrees of freedom motions were solved in the time domain, taking account of all forces acting on the body. Integration yielded motions, accelerations, velocities, and translational and rotational displacements.

After updating the position of the ship and again computing the fluid flow for the new position and integrating over time, the trajectory of the ship was obtained.

The equations of motion were solved in the Newtonian reference frame (G,x,y,z) fixed with respect to the mean position of the ship. Its origin was located at the center of gravity of the ship, G. The coordinate transformation between the Newtonian and the ship-fixed local reference frame (G,ξ,η,ζ) was defined as follows:

$$\vec{x} = \vec{x}_G + S\vec{\xi}$$

where S denotes the transformation matrix and $\vec{\xi}$ the rotational position vector. The transformation matrix resulted from consecutive rotations about the vertical z-axis (yaw), the new transverse η-axis (pitch), and the new longitudinal ξ-axis (roll). The governing equations of motions are expressed as follows:

$$\vec{F} = m \cdot \ddot{\vec{x}}_G$$

$$\vec{M} = S\, I_L S^T \dot{\vec{\omega}} + \vec{\omega} \times S\, I_L S^T \vec{\omega}$$

where $\vec{F}$ denotes the resulting force vector, m the mass of the ship, $\ddot{\vec{x}}_G$ the translational acceleration vector of G, $\vec{M}$ the resulting moment vector with respect to G, I_L the inertia tensor of the ship about the axes of the ship-fixed (local) reference frame, and $\vec{\omega}$ the angular velocity vector. Integration in the time domain relied on the use of the so-called explicit trapezoidal method, Brunswig and El Moctar, 2004).

We validated motion predictions of the extended RANSE solver by comparing computations with experimental measurements obtained

from systematic model tests performed at the Hamburg Ship Model Basin (HSVA). These tests were carried out at a scale of 1:13, albeit not for a model of one of the ships investigated here, but for a 100 m motor yacht of 3600 t displacement. The favorable agreement between experimental measurements and RANSE computations validated the extended RANSE solver. Sample time histories of measured pitch , roll motion and vertical acceleration at the yacht's forward perpendicular (FP) are shown in Fig. 1 together with comparable results obtained from RANSE computations.

FLOW AND MOTION SIMULATION

The numerical volume grids surrounding the ships comprised typically between one and three million hexahedral control volumes. To avoid flow disturbances at outer grid boundaries, these boundaries were located one ship length ahead of the bow, two ship lengths aft of the stern, one ship length beneath the keel, and one ship length above the deck. This large domain of the mesh, especially above the deck, was necessary to allow large pitch motions in head waves. Near the ship hull and at the inlet boundary of the waves, grid density was high to resolve the wave, whereas at the outlet boundary of the waves, grid density was relatively course in order to dampen the waves. The innermost dimensionless cell thickness was chosen such that n+ = 100 on average. Figure 2 shows the numerical grid on the surface of the containership.

Front, side, bottom, and top flow boundaries were specified as inlets of known velocities and known void fraction distributions, thereby defining water and air regions. On the hull surface a no-slip condition was enforced on fluid velocities and the turbulent kinetic energy. The wake flow boundary was specified as a zero-gradient pressure boundary (hydrostatic pressure). All computations were performed using the RNG-k-ε turbulence model with wall functions. The time step size was chosen such that the Courant number was smaller than unity on average. Time step size was typically between 0.01 s. Ship motions were realized by moving the entire grid at each time step. Thus, all boundary conditions were newly computed at each time step.

Volume fractions and velocities that initialized the flow field arose from the superposition of ship speed and orbital particle velocities of the waves. Numerical diffusion caused by the course grid aft of the ships dampened the incident wave to such an extent that no significant wave reflection occurred at the outlet boundary.

Simulation of the flow fields continued until reaching a periodic solution. After a simulation time of two to five encounter periods, depending on ship motions, ship speed, and wave height, periodically converging solutions were obtained. For each time step up to ten outer iterations were needed.

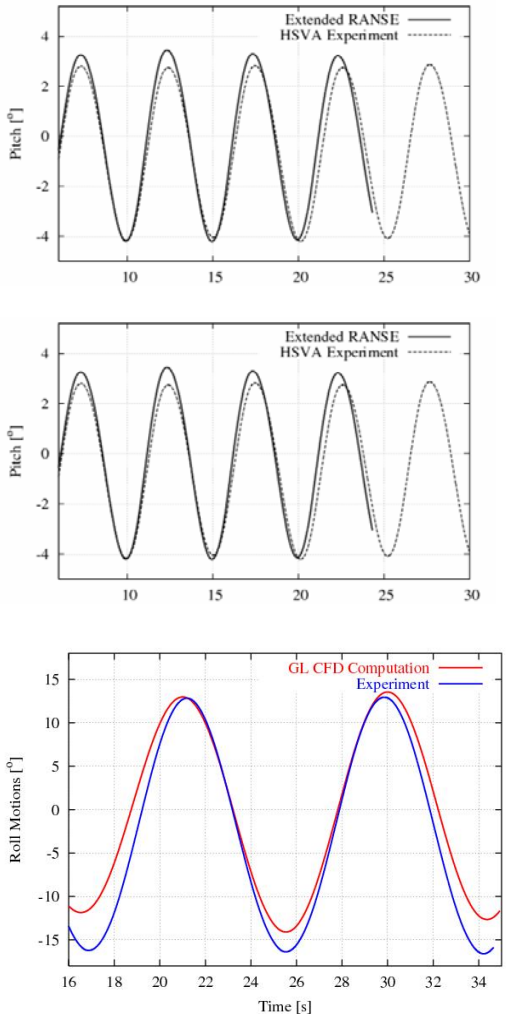

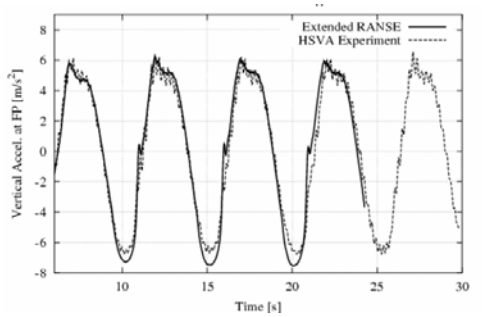

Fig. 1: Comparative time histories of pitch, roll motion and vertical acceleration at FP for a motor yacht in head and oblique regular waves

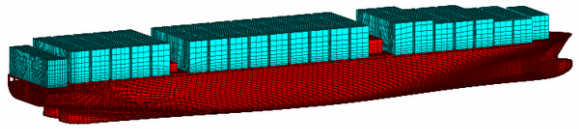

Fig. 2**:** Numerical grid on surface of the containership

LARGE POST-PANMAX CONTAINERSHIP

El Moctar et al. (2004, 2006) present in detail results of nonlinear seakeeping analyses for three hulls, with a focus on slamming and global loads. One of these hulls is a large modern Post-Panmax Containership. The sectional loads of a large modern Post-Panamax containership were computed for design wave conditions using RANSE and the frequency-domain panel code (GLPANEL). Non-linear corrections were applied to the GLPANEL computed loads.

The critical wave conditions selected represented worst case scenarios for midship vertical bending moment. Head wave conditions were rated most critical from the standpoint of slamming loads on the bow. However, because of the extreme stern overhang characteristic of modern containerships, stern wave conditions were also studied.

In heavy seas, the added resistance tends to result in voluntary or involuntary speed loss. Thus, both ships were analyzed advancing at reduced speeds. The exact speed loss was difficult to establish. Therefore, several reduced forward speeds were considered.

Table 1 shows main data of the containership and the design wave.

Wave-induced sectional loads were computed for the ship advancing at one-third and two-third forward speed in the design wave. For this particular case, the hull girder was subject to a vertical still-water sagging moment. Figures 3 to 6 depict the corresponding envelope curves of maximum and minimum vertical bending moments and shear forces at sections along the length of the ship. Results show that at one-third forward speed, sectional loads from RANSE compared favourably with sectional loads from GLPANEL. However, at two-third forward speed, bending moments as well as shear forces differed significantly in the bow region. These differences were caused by the effects of slamming at the bow and green water on deck, see Fig.7. As expected, these effects were more pronounced at higher forward speed. The results demonstrate the importance of accounting for the ship's forward speed when computing wave-induced sectional loads.

Table 1 : Principals particulars of Post-Panamx Containership

Length [m]	330
Width [m]	48
Draft [m]	12
Speed [kts]	27

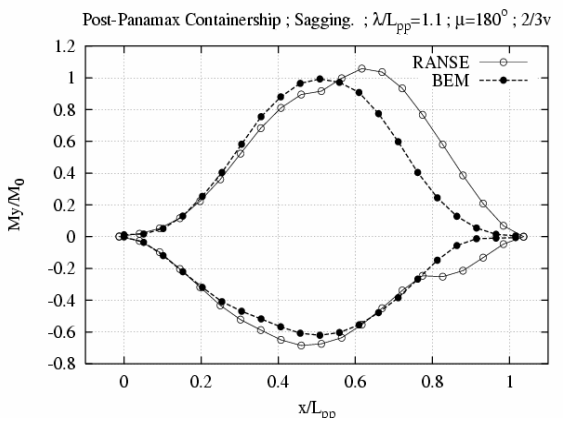

Fig.3: Envelopes of vertical bending moments for 2/3 ship speed at midship design wave condition

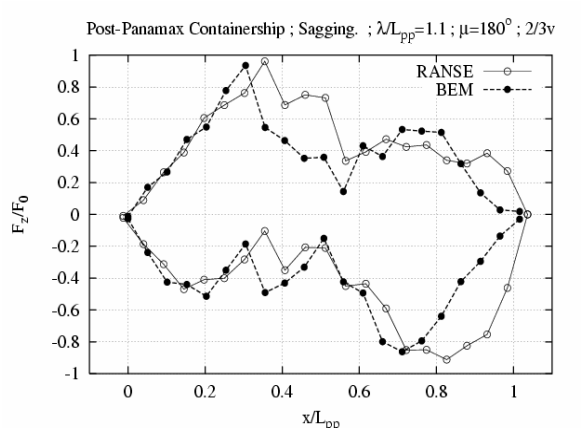

Fig.4: Envelopes of vertical shear forces for 2/3 ship speed at midship design wave condition

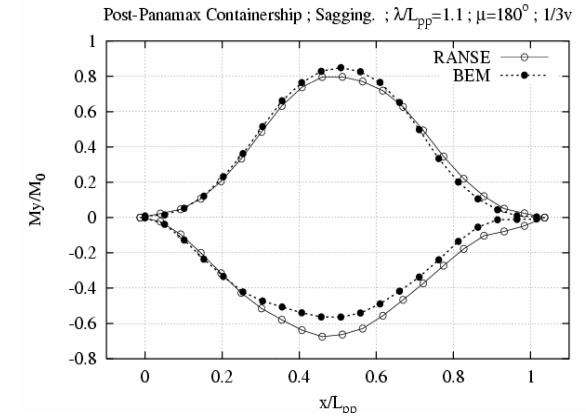

Fig.5: Envelopes of vertical bending moments for 1/3 ship speed at midship design wave condition

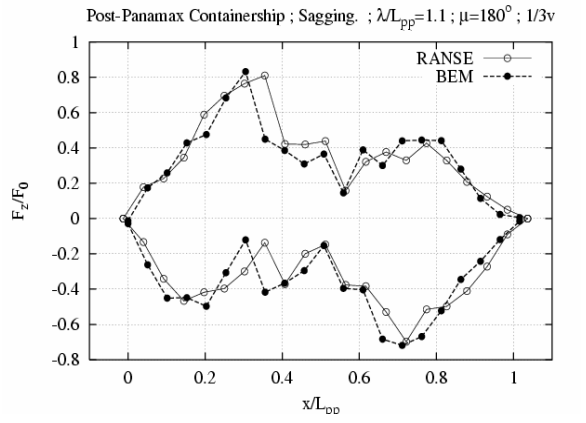

Fig.6: Envelopes of vertical shear forces for 1/3 ship speed at midship design wave condition

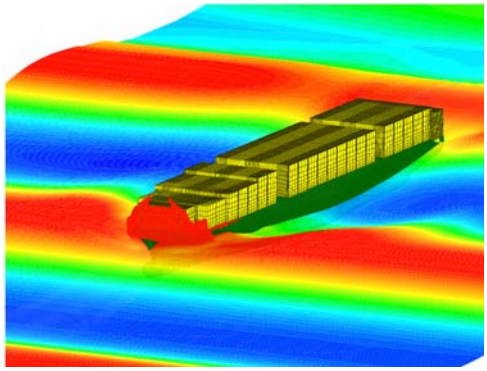

Fig.7: Water on deck of the containership

'ERTHRACE' TRIMARAN

EARTHRACE is a wavepiercing trimaran designed to break the world record for global circumnavigation using only renewable fuels. Circumnavigating the globe represents the world's longest marine race, spanning some 24,000 nautical miles. The current record stands at 75 days. Germanischer Lloyd was asked to assess the hydrodynamic loads and the ship motions. Figure 8 shows a pictorial representation of EARTHRACE, and Table 2 lists its principal particulars.

The unconventional shape of EARTHRACE represents a completely new design for which no rules are available. In addition, the vessel's extremely high service speed relative to its size (Froude number in access of 1.7) as well as its complex geometry made it necessary to account for forward speed effects and large (finite amplitude) waves. At sea, part of the ship's hull is likely to be completely immersed by waves, causing large amplitude highly nonlinear ship responses, and wave impact-related (slamming) loads had to be accounted for as well. This meant that standard potential flow based seakeeping analysis methods were unsuitable.

Screen shots of EARTHRACE in head and oblique waves, shown in Fig. 9 and pressure distributions, shown in Fig. 10, are typical samples of computed results.

Three cases that represent worst-case design scenarios were investigated. The first three cases determined design loads for the vessel advancing at 25 kts speed in waves of different

amplitude, period, and heading. These loads were later used as inputs for a structural analysis.

Figures 11 and 12 show typical time histories of computed results, here for case 1, examining the trimaran advancing at service speed of 25 knots in 5.0m high regular head waves. As seen in Fig. 11, maximum heave and pitch motions turned out to be 1.5m and 15°, respectively, and the corresponding maximum vertical acceleration reached values up to 2.25 times the acceleration of gravity. The corresponding hydrodynamic loads acting on one of the sponsons are shown in Fig. 12. These time histories revealed a typical characteristic of the vessel's motion behavior, namely, the response amplitude alternated between two values. This was the case although the amplitude of the incident wave train remained the same. Such highly nonlinear behavior occurred in large amplitude head waves. The ship's first encounter with such a large amplitude wave caused its entire foreship to be immersed into the surrounding water. The resulting initial conditions of the ship when it then headed into the following wave were not like those of the first wave and, consequently, the ship's response differed from the response caused by the first wave. This process more or less repeated itself during the next two wave amplitudes.

Cases 2 and 3 investigated the vessel's response in regular waves of lesser height and length, but again at the design speed of 25 knots. Motions, accelerations, and hydrodynamic loads were found to be less than for case 1. However, the largest hydrodynamic pressure occurred in oblique waves.

Fig. 8: The wavepiercing trimaran EARTHRACE

Table 2: Principal particulars of

EARTHRACE	
Displacement	24,900 kg
Length overall	23.9 m
Breadth at design waterline	7.9 m
Draft, full load	0.91 m
Service speed	25/50 kts

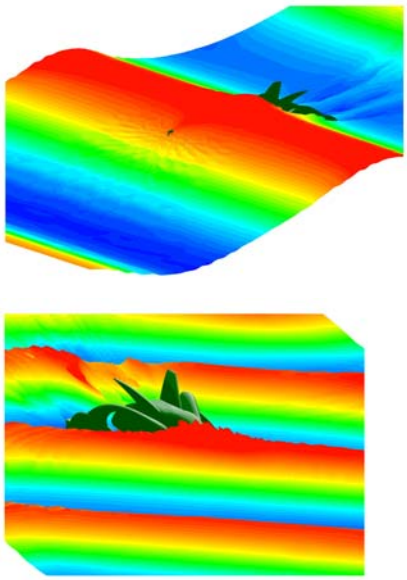

Fig.9: Trimaran in head and oblique regular waves

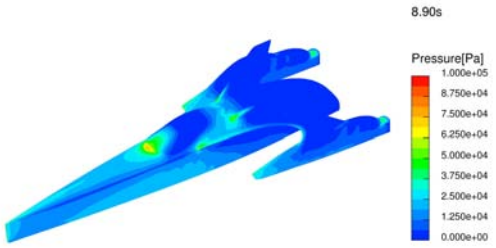

Fig.10: Pressure distribution on Trimaran

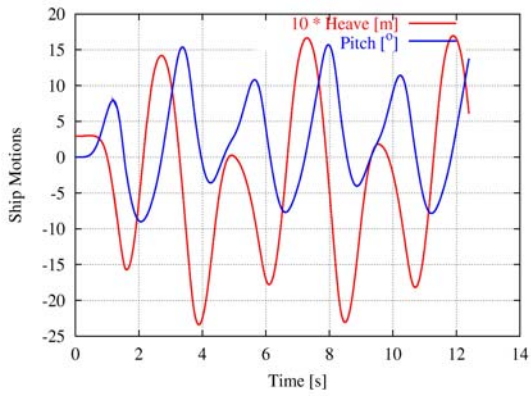

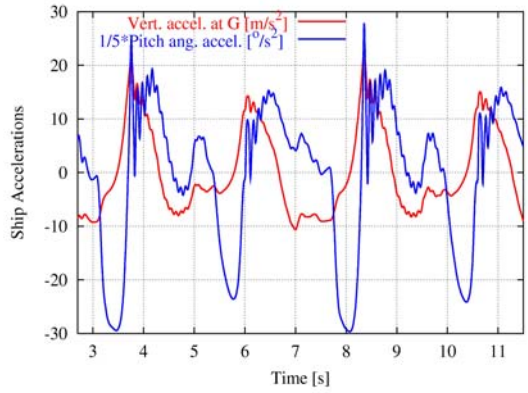

Fig.11: Motions and accelerations of EARTHRACE in 5.0m high head waves

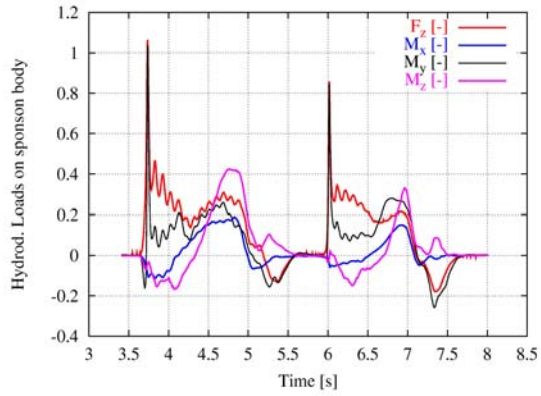

Fig.12: Normalized hydrodynamic forces on a sponson of EARTHRACE in 5.0m high head waves

CONCLUSIONS

Potential flow solvers remain useful in seakeeping analysis. However, for large ship motions (capsizing) and large loads (slamming), modern free-surface RANSE solvers offer superior simulation capability. Inclusion of green water on deck (or internal flooding) directly coupled to the global motions of the ship are feasible by now, with virtually no restrictions on ship or wave geometry. While the applications shown here focussed largely on loads on the ship, the same approach could be used for advanced capsizing simulations. For some time to come, such simulations will be restricted to a few service providers, as they require considerable resources in hardware, software and skill in using sophisticated programs for grid generation and simulation.

REFERENCES

Blume P., Ship Technology Research 26, Experimentally determined coefficients for effective roll damping and application to estimate extreme roll angles, 1979 (in German)

Brunswig J., El Moctar, O., 7th Numerical Towing Tank Symposium (NuTTS), Hamburg, Prediction of ship motions in waves using RANSE, 2004

Brunswig, J. Pereira, R., Kim, D-W. "Validation of parametric roll motion predictions for a modern containership design, Proc., 9th Int. Conf. on Stability of Ships and Ocean Vehicles STAB'2006", Proceedings of the International , Conference on Fast Sea Transportation (STAB), Rio, 2006

El Moctar O.M., Brehm A., Schellin T., 25th Symp. Naval Hydrodynamics, St. John's, Prediction of slamming loads for ship structural design using potential flow and RANSE codes, 2004a

El Moctar O.M., Schellin T., Priebe T., 26th Symposium on Naval Hydrodynamics, Rome, CFD and FE methods to predict wave loads and ship structural response, 2006

El Moctar, O., Brunswig, J. Brehm ,A., Schellinn, T.E. "Computation of Ship Motions in Waves and Slamming Loads for Fast Ships using RANSE", Proceedings of the International , Conference on Fast Sea Transportation (FAST), St. Petersburg, 2005

Pereira, R. (1988) Simulation nichtlinearer Seegangslasten, Schiffstechnik 35(4) 173-193

Papanikolaou A., Schellin T.E., J. Ship Technology Research Vol. 39, A three-dimensional panel method for motions and loads of ships with forward speed, pp.147-156, 1991

Söding, H. Leckstabilität im Seegang. Report No.429, Institut für Schiffbau, 1982